RESEARCH ARTICLE
doi: 10.2306/scienceasia1513-1874.2023.012

ScienceAsia 49 (2023): **282–289**

Stress relaxation behavior and effects of accelerated weathering on properties of silane-treated rubberwood/recycled polypropylene wood-plastic composites

Thanate Ratanawilai[a,*], **Sriwan Khamtree**[b], **Sukritthira Ratanawilai**[c]

[a] Smart Industry Research Center, Department of Industrial and Manufacturing Engineering, Faculty of Engineering, Prince of Songkla University, Hat Yai, Songkhla 90110 Thailand
[b] Faculty of Industrial Technology, Songkhla Rajabhat University, Songkhla 90000 Thailand
[c] Department of Chemical Engineering, Faculty of Engineering, Prince of Songkla University, Hat Yai, Songkhla 90112 Thailand

[*]Corresponding author, e-mail: thanate.r@psu.ac.th

Received 30 Jul 2021, Accepted 4 Nov 2022
Available online 9 Feb 2023

ABSTRACT: Silane-treated rubberwood flour (RWF) was mixed with recycled polypropylene (rPP) at the optimum proportions of 39.22 wt% RWF content and 60.78 wt% rPP, with the RWF being silane-treated at a 3.44% concentration based on the weight of RWF. These materials were mixed to produce wood-plastic composites (WPCs) using twin-screw extrusion followed by hot pressing. The objective of this study was to investigate the stress relaxation behavior and the effect of accelerated weathering on the mechanical properties of the produced WPCs. The results show that stress relaxations at different temperatures with constant strain levels were consistent, and the stress decreased with time. In addition, the stress relaxation rate increased with strain level at a constant temperature. Time-temperature superposition was applied to construct a master curve extension for 1.0, 1.5, and 2.0% strain levels over 208, 187, and 75 days, respectively. The results indicate that the WPCs were rheologically simple materials, and a single horizontal shift of the time axis was adequate to predict their long-term responses. Moreover, accelerated weathering tests of the WPCs indicate that accelerated weathering had no significant effect on the mechanical properties of WPCs.

KEYWORDS: stress relaxation, accelerated weathering, silane, rubberwood flour, polypropylene

INTRODUCTION

Wood-plastic composites (WPCs) are mainly composed of natural wood and plastic. They are produced as a substitute for natural wood and could be made of wood waste and recycled plastic to produce an ecologically friendly material. Wood, such as palm, spruce, pine, fir, eucalyptus, oak, or rubberwood [1–4], could be used as a reinforcing filler in a polymer matrix to improve its mechanical properties; for example, the modulus and the strength [5]. Polypropylene (PP) is among the most often used types of polymer in WPCs. They are widely used in many applications such as outdoor decking, railings, fences, doors, and window frames; and also in the manufacture of furniture. Although several studies have been conducted to investigate the effects of various factors on physical, mechanical, and thermal properties of WPCs; the time-dependent properties of these materials were seldom been discussed [6, 7]. Moreover, concerns have been raised about the use of WPCs in outdoor applications, specifically about their resistance to weathering [8, 9]. Their vulnerability to stress relaxation and creep in long-term applications is also of particular interest [5].

Stress relaxation and creep are the two phenomena tested to predict the long-term mechanical performance of a composite [10]. Stress relaxation refers to the reduction in stress with time in response to constant strain of the material [11–13]. In previous studies, temperature, wood content, and strain level have been found to affect the stress relaxation behavior of WPCs, which has been noted to occur at a faster rate at elevated temperatures [11, 14–16]. As an exception, a decrease in the relative stress with increasing temperature was found in Chinese white poplar veneer [17]. In addition, the wood content has been found to exert a great influence on the stress relaxation behavior of WPCs; i.e., rate of stress relaxation decreases with higher wood content [11, 14]. Wang et al [7] reported that the lowest stress relaxation rates appeared at a 40% wood content in WPCs, while Pothan et al [18] also found that 40% banana fiber in a polyester matrix minimized the rate of relaxation; and in addition, treating the banana fiber with sodium hydroxide was contributed to the lowest rate of stress relaxation.

The effects of natural and accelerated weathering on the physical and mechanical properties of WPCs lead to discoloration and photodegradation of their surfaces, and a number of studies have reported that outdoor natural weathering occurs over time [19–21] and impacts the flexural strength of WPCs, which have been found to be degraded after one year. Therefore, several studies have focused on the effects of accelerated weathering on tensile, flexural, and impact properties. Turku and Karki [22] found that the tensile properties of WPCs were degraded after accelerated

weathering for 164 h, and loss of flexural and impact properties of WPCs after accelerated weathering has been reported from several studies [8, 23, 24].

A review of the literature reveals that temperature, UV light, and moisture can affect WPCs, contributing to creep and stress relaxation which may lead to changes in the physical and mechanical properties of WPCs when used over long periods. Therefore, the objective of this study was to investigate the stress relaxation behavior and the effects of accelerated weathering on the mechanical properties of the produced WPCs. The testing of the stress relaxation behavior was conducted under a constant strain at various temperatures. The influences of the strain level and temperature were investigated to construct master curves and to predict the long-term stress relaxation behavior of the WPCs by using the time-stress superposition technique. Moreover, an accelerated weathering test was conducted to investigate the effects on physical and mechanical properties of the WPCs.

MATERIALS AND METHODS

Raw materials

Recycled PP (rPP) pellets with a melt flow index of 11 g/10 min at 230 °C were obtained from Withaya Intertrade Co., Ltd., Samutprakarn, Thailand. Rubberwood flour (RWF) used as a reinforcer in the composites was obtained in the form of sawdust from a local furniture factory in Trang, Thailand. The sawdust was passed through an 80-mesh sieve. Sodium hydroxide (NaOH) and triethoxyvinylsilane (97%) were purchased from Merck, Germany, and from Sigma-Aldrich, USA, respectively.

The RWF was treated with NaOH solution (2% w/v) at 25 °C for 24 h and was then washed with distilled water until it became neutral, followed by drying in a hot air oven at 80 °C for 24 h. Silane at 3.44%, was dissolved in ethanol and water (50:50 v/v). The pH of the silane solution was maintained between 4.5 and 5 by adding acetic acid, and stirring at room temperature for 1 h. The alkaline treated RWF was immersed in the silane solution for 2 h before filtering and drying in a hot air oven at 80 °C for 24 h [25, 26].

Preparation of wood-plastic composite sample

The rPP pellets and treated RWF were mixed, by using a twin-screw extruder (Model EMT-26 from En Mach Co., Ltd., Nonthaburi, Thailand), to obtain a composite sample with an RWF content of 39.22% by weight, which was the optimum conditions for physical and mechanical properties of the composite samples suggested by Khamtree et al [27]. The temperature zones of the extruder were controlled at 160–190 °C with the screw rotation speed set at 60 rpm. The extruded compound was cut and molded in a hot compression molding machine with the dimensions of 160 mm × 245 mm × 4 mm (width × length × thickness) at 190 °C under 1000 psi pressure for 15 min and then cooled to room temperature under 500 psi pressure for 10 min.

Stress relaxation

The stress relaxation test was performed using a 100 kN load cell of Instron Universal Testing Machine (Model 5582, Instron Corporation, Massachusetts, USA) in three-point flexural mode and following ASTM D 790-92 with the dimensions of the sample of 13.5 mm × 130 mm × 4 mm (width × length × thickness). The crosshead speed was 2 mm/min, and the span length was fixed at 80 mm. The strain was held constant after the required level was reached, and the delayed response in stress were recorded as a function of time for 3600 s. The samples were tested at three strain levels: 1.0, 1.5, and 2.0%. The tests were performed at temperatures of 25, 40, 50, and 60 °C. The experiment was conducted in three replicates for each condition. The stress decay was calculated as $\sigma(t)/\sigma(0)$, where $\sigma(0)$ is the initial stress at zero time ($t = 0$), and $\sigma(t)$ is the stress at subsequent times. The stress decay was recorded starting at 1 s after the predetermined strain was attained. Time-temperature superposition principle, a relationships between stress and time, was applied to the master curve. The stress relaxation curve at 25 °C was considered as a reference state, and the other curves at 40, 50, and 60 °C were shifted horizontally to construct the master curve. It is a characteristic of polymers that stress relaxation occurs at a progressively decreasing rate with time. The power-law model of stress relaxation is given by:

$$\sigma(t) = \sigma_s \left(\frac{t}{t_s} \right)^{-n} \tag{1}$$

where σ_s is the specific stress, n is a constant fitted to the experimental data and normally less than one and negative, and t_s is the specific time simply used to non-dimensionalize the time variable, a constant normally taken as 1 s.

Accelerated weathering

The weathering tests on the samples were performed following ASTM G154 (2016) cycle type I, using a QUV-accelerated weathering tester (QUV spray, Q-lab Corporation, USA). The conditions of the QUV-accelerated weathering aging test included UVA radiation at a wavelength of 340 nm and an intensity of 0.89 W/m^2 at 60 °C for 8 h, and water-condensation at 50 °C for 4 h. The total aging time was 7 days.

Physical and mechanical properties

The surface color of the composite samples before and after accelerated weathering was measured with a Hunterlab Color Standard (Hunter Associates Laboratory, Inc., Virginia, USA). The CIELAB color system

was used to report the surface color in L^*, a^*, b^* coordinates where L^* represents the lightness and varies from 100 (white) to 0 (grey); a^* represents color components from red ($+a^*$) to green ($-a^*$); and b^* represents components from yellow ($+b^*$) to blue ($-b^*$). There were ten replications of each test. The color difference or discoloration (ΔE) was calculated as follows:

$$\Delta E^* = \sqrt{(\Delta L^*)^2 + (\Delta a^*)^2 + (\Delta b^*)^2} \qquad (2)$$

Where ΔL^*, Δa^*, Δb^* and represent the component differences between before and after weathering, in respective coordinates L^*, a^*, and b^*.

Measurements of the composite's hardness were performed according to ASTM D 2240 using two durometers both employing the Shore D scale. The dimensions of the samples were 25.4 mm × 25.4 mm × 4 mm (width × length × thickness). The hardness of individual samples was measured at five locations for each experimental condition. Measurements of the tensile and flexural properties were performed according to ASTM D 638-91 and ASTM D 790-92, respectively, using the same Instron Universal Testing Machine (Model 5582) used to measure the stress responses. The tensile properties were determined with a testing speed of 5 mm/min. Three-point flexural properties were measured at a crosshead speed of 2 mm/min. All experiments were performed at room temperature with ten replications.

RESULTS AND DISCUSSION

Effect of temperature on the stress relaxation behavior of composite samples

The plots of stress ratios $\sigma(t)/\sigma(0)$ against time at temperatures of 25, 40, 50, and 60 °C and at strain levels of 1.0, 1.5, and 2.0% were shown in Fig. 1(a-c). The results show that the trend in stress at a constant strain level was consistent across all cases; i.e., decreasing with time. Moreover, the stress relaxation curves were more obvious when rate of stress relaxation was higher at higher temperatures and constant strain. This finding is in agreement with those of Bhattacharyya et al [14] and Cao et al [28]. With increasing temperature, the polymers have higher molecular energy, and the free volume in the material becomes larger, which finally results in the breakage of bonds and, hence, the acceleration of stress relaxation [11].

The rate of stress relaxation was defined as the slope in a log-log plot of $\sigma(t)/\sigma(0)$ vs. time. For relaxation times up to 1000 s, there was only little deviation from linearity [7, 15]. Therefore, the rates of stress relaxation (and the values of R^2) were calculated to investigate the effects of temperature and strain level on the flexural relaxation rate of the composite samples, and the results were shown in Table 1. The rates of stress relaxation at 2.0% strain were 0.071, 0.114, 0.158, and 0.313 at temperatures of 25, 40, 50, and 60 °C, respectively. The coefficients of determination R^2 were very close to 1, indicating good linearity in the log-log plot of stress versus time [7, 15] (Fig. 2). The rate of stress relaxation increased with temperature because of the homogeneous interfacial structure and weak compatibility between the RWF and rPP [15]. This result is in a good agreement with

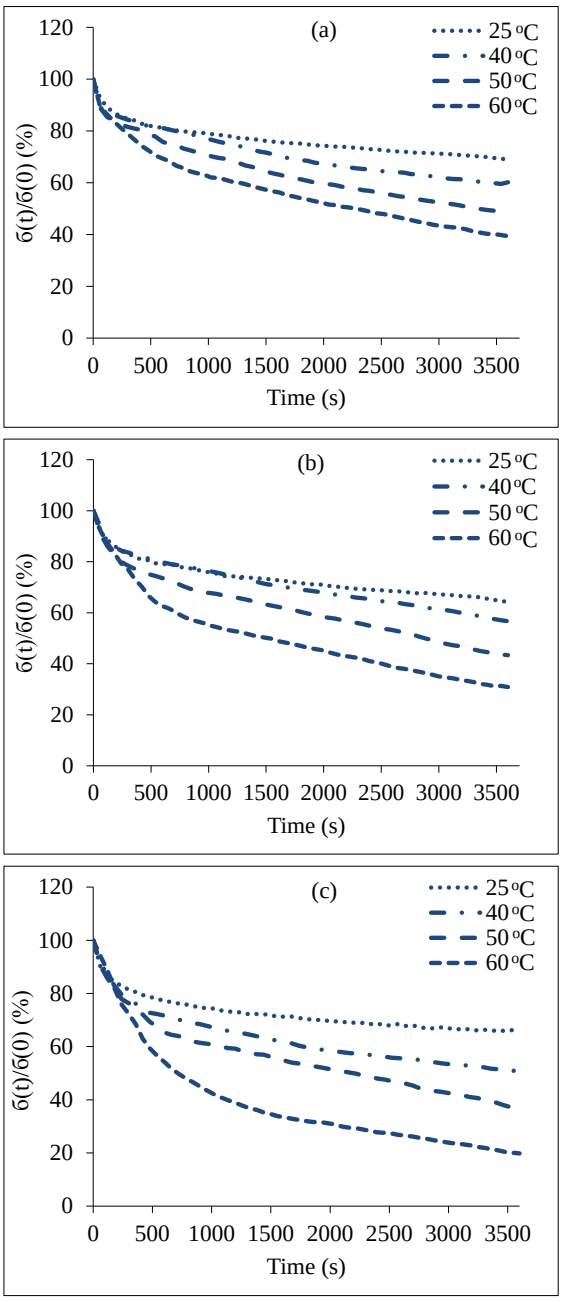

Fig. 1 Flexural stress relaxation of WPCs at different strains: (a), 1.0%; (b), 1.5%; and (c), 2.0%; at tempertures of: 25 °C, 40 °C, 50 °C, and 60 °C.

Table 1 Rates of flexural stress relaxation of WPCs.

Strain (%)	Rate of stress relaxation (negative)			
	25 °C	40 °C	50 °C	60 °C
1.0	0.057 (0.99)	0.060 (0.96)	0.088 (0.89)	0.142 (0.99)
1.5	0.068 (0.99)	0.068 (0.99)	0.106 (0.98)	0.205 (0.95)
2.0	0.071 (0.99)	0.114 (0.99)	0.158 (0.97)	0.313 (0.94)

† The values in parentheses are the R^2 values of linear regression which fit to log−log plots of $\sigma(t)/\sigma(0)$ versus t (10–1000 s)

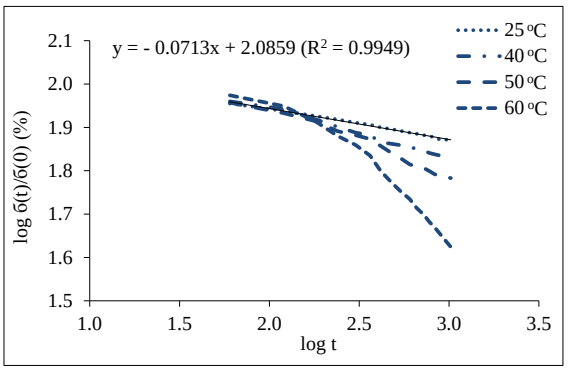

Fig. 2 log-log plots of the relative stress versus time for WPCs at 2.0% strain and temperatures of: 25 °C, 40 °C, 50 °C, and 60 °C.

Wang et al [11]. Moreover, the stress relaxation of WPCs showed that the stress relaxation was reduced with time. The reduction of ralaxation rates of the RWF treated with alkali and silane was due to an improved adhesion between fiber and matrix [18]. However, for the WPCs treated with silane, the bonding of silanol from the silane and the hydroxyl groups of the cellulose leads to the scission of bonds established between the fiber and the matrix. Moreover, the stress relaxation was affected only after longer periods of time. The bond scission occurs, and the deformable layer retracts, which is felt as the increased decay in stress [18]. This result is in consistent with Yang et al [7], who concluded that addition of MAPP to the composite would increase the internal bonding, resulting in the slow stress relaxtion. In addition, the result is also in agreeable with Pothan et al [18], who reported that the relaxation rate of fibers treated with alkaline and silane, compared with unterated glass fibers, was reduced due to an improved adhesion.

Effect of strain on the stress relaxation behavior of composite samples

Fig. 3 shows the relative flexural stress during relaxation $\sigma(t)/\sigma(0)$ as a function of time for different strain levels. It can be clearly seen from Fig. 3(a) that the composite samples at 25 °C with different strains of 1.0%, 1.5%, and 2.0% experienced comparatively slow stress relaxation. This result is similar to those of Younes and Rahman [6] and Obaid et al [5], who concluded that stress relaxation decreased with time under a constant strain. The stress relaxation curves at 40, 50, and 60 °C were rather similar, as can be seen from Fig. 3(b-d), respectively.

Table 2 Power-law models as master curves for stress relaxation at different strain levels.

Strain (%)	Power-law model	R^2
1.0	$46.537t^{-0.139}$	0.9448
1.5	$66.733t^{-0.153}$	0.9024
2.0	$93.243t^{-0.184}$	0.9047

The rate of stress relaxation increased with strain level, at a constant temperature. Table 1 shows that the rate of stress relaxation obtained at 2.0% strain was higher than that with 1.5 or 1.0% strain. At 60 °C, the rates of stress relaxation at 2.0, 1.5, and 1.0% were 0.313, 0.205, and 0.142, respectively. The higher rate of stress relaxation at a higher strain level could be explained by more permanent changes occurring in the material, and the material is deformed at a higher strain rate which will be reversible and elastic [29]. Moreover, the strain enhances the probability of a chain segment possessing enough energy to flow; and, as a result, more viscos flow takes place [30]. This result is in a good agreement with Mirzaei et al [31], who reported that higher stress relaxation rate corresponds to a higher applied strain level.

The master curve for composite samples at room temperature

The stress relaxation behavior of the composite samples with a 2.0% strain level at different temperatures was shown in Fig. 4. Applying the time-temperature superposition principle, the stress relaxation curve at 25 °C was considered as a reference state, and the other curves were shifted horizontally to construct the master curve shown in Fig. 5. The curves for strain levels of 1.0% and 1.5% were similar to the master curve for 2.0% strain level.

The master curve of the stress relaxation obtained for the composite samples at 2.0% strain level was shown in Fig. 6. At 2.0% strain level, the 60 min stress relaxation data were extrapolated up to 108,000 min (75 days) by extent of the revised master curve. In

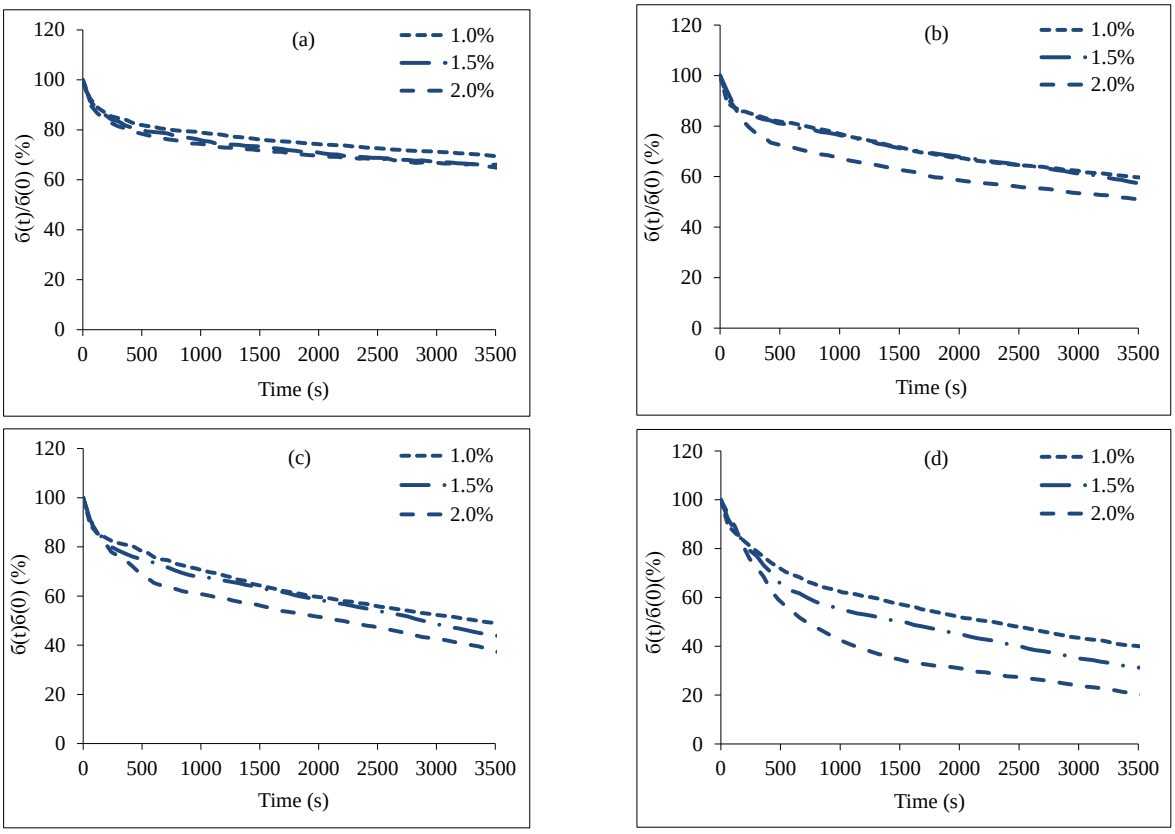

Fig. 3 Flexural stress relaxation of WPCs at temperatures of: (a), 25 °C; (b), 40 °C; (c), 50 °C; and (d), 60 °C; at strain levels of: 1.0, 1.5, and 2.0%.

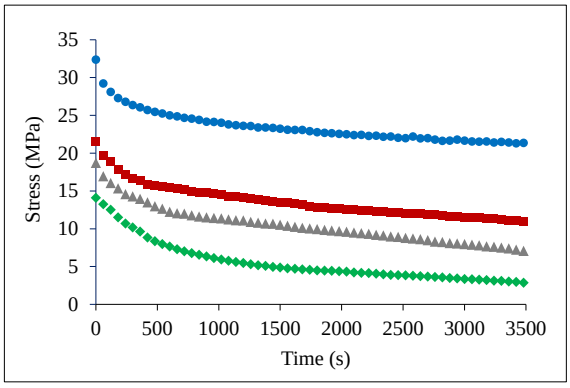

Fig. 4 Flexural stress relaxation of WPCs with 2.0% strain level at different temperatures of: ●, 25 °C; ■, 40 °C; ▲, 50 °C; ♦, 60 °C.

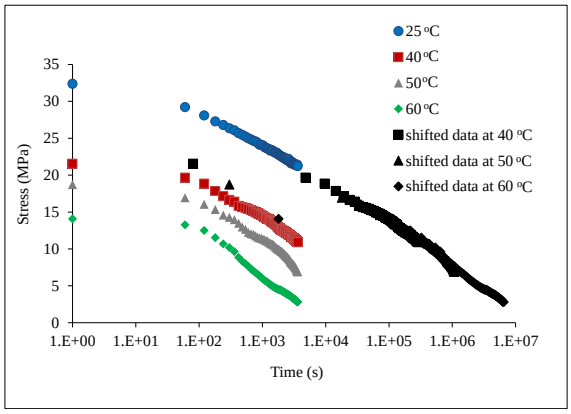

Fig. 5 The horizontal shifted curves for stress relaxation at 2.0% strain to overlay cases measured at different temperatures.

addition, the data for 1.0% and 1.5% strain levels for 60 min stress relaxation were extrapolated up to 208 days and 187 days, respectively. The power-law parameters and R^2 of the master curves for stress relaxation were calculated (Table 2). The R^2 values obtained for the equations for the 1.0, 1.5, and 2.0% strain levels were 0.9448, 0.9024, and 0.9047, respectively. The results were similar to those of Siengchin et al [16], in which the power-law fitted very well with the stress relaxation behavior. Thus,

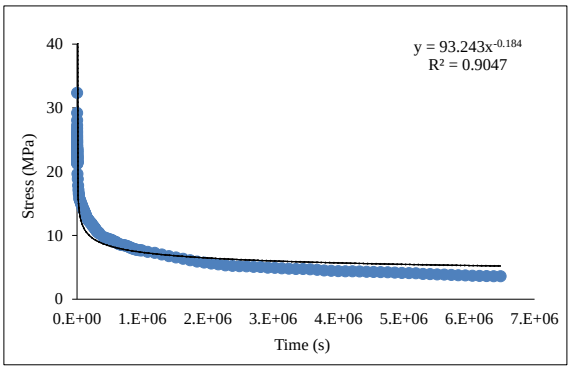

Fig. 6 The master curve for stress relaxation at 2.0% strain.

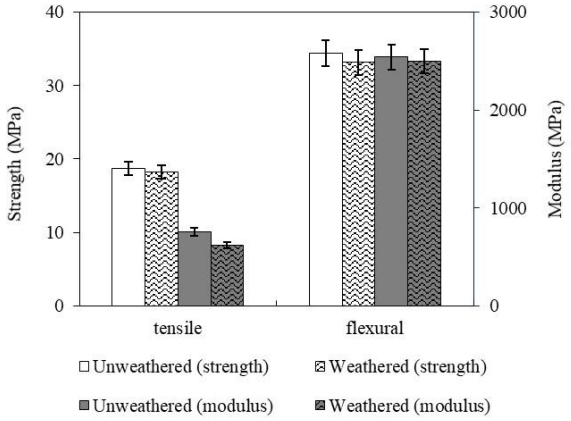

Fig. 7 Mechanical properties of WPCs before and after accelerated weathering.

Table 3 Effects of accelerated weathering on the physical properties of WPCs.

Physical property	Unweathered	Weathered	% change
L^*	19.49 (0.30)	54.70 (0.61)	35.21
Hardness	76.20 (0.42)	75.60 (0.23)	–0.79

† The values in parentheses are standard deviations from ten replicates.

the long-term stress relaxation of the WPCs at different strain levels can be reliably predicted using the power law model.

Additionally, to confirm the estimates of stress relaxation behavior, 3 replications were conducted at 2.0% strain and 25 °C for 5 days. The master curve and experimental results were compared, and the root mean square error (RMSE) was 6.98, indicating a good match of the power-law model with the prolonged experiments.

Color analysis

The composite samples became comparatively light in color after accelerated weathering. The color coordinate L^* and the color difference or discoloration (ΔE) were investigated, and the results were shown in Table 3. The results show that the (L^*) of the composite samples increased by approximately 35.21% during accelerated weathering, caused by photodegradation of the RWF and by other structural changes [32, 33]. This result is in a good agreement with that of Chaochanchaikul et al [34], who reported that composites exposed to QUV weathering for 240 h experienced a change in L^* by approximately 50%. A ΔE of 35.35% was observed for the composite samples when exposed to accelerated weathering, indicating bleaching of the RWF component, degradation of the polymer due to UV radiation, with a darkening effect possibly linked to surface oxidation [8].

Hardness analysis

The result of hardness of the composite samples before and after accelerated weathering was shown in Table 3. The composite samples suffered a reduction of the hardness by approximately 0.79% due to polymer chain scission, which resulted in surface cracks and embrittlement [19]. Moreover, the effects of accelerated weathering on hardness were also verified by statistical analysis (t-test). The hardness decreased significantly (p-value < 0.05) during accelerated weathering. However, adding a UV stabilizer to the WPCs has been found to reduce the loss of hardness caused by weathering [19].

Mechanical properties of composite samples

The results of tensile and flexural properties of the composite samples before and after accelerated weathering in Fig. 7 showed that all properties of the composite samples were degraded by accelerated weathering, probably due to the decreased crystallinity of the polymer matrix [35]. The tensile strength and modulus decreased from 18.68 MPa and 755.19 MPa to 18.28 MPa and 620.64 MPa, respectively. In addition, the flexural strength and modulus dropped from 34.41 MPa and 2542.67 MPa to 33.14 MPa and 2495.83 MPa, respectively. Similar trends, i.e. degraded mechanical properties of WPCs from accelerated weathering, have been reported by several previous studies [8, 9, 19, 35].

The effects of accelerated weathering on mechanical properties were also verified by statistical analysis (t-test). The tensile and flexural properties of the composite samples were not significantly ($p > 0.05$) affected by weathering. The p-values of changes in tensile strength, tensile modulus, flexural strength, and flexural modulus were 0.552, 0.393, 0.092, and 0.644, respectively.

CONCLUSION

This study investigated the stress relaxation and the effects of accelerated weathering responses of wood-plastic composites samples containing silane-treated RWF. The stress relaxation rate increased with temperature and strain level, and decreased from the initial rate with time. Furthermore, a master curve was constructed by horizontal shifting of curves for various temperatures to overlay them. At all strain levels, the stress relaxation behavior exhibited similar trends, and the long-term behavior of the composite samples can be predicted using the equations derived. In addition, the mechanical properties results of the composite samples showed that the tensile and flexural properties were not significantly affected by accelerated weathering.

Acknowledgements: This work was supported by the Smart Industry Research Center, Department of Industrial and Manufacturing Engineering, Faculty of Engineering; the Rubberwood Technology and Management Research Group [grant number Eng-54-27-11-0137-S], Faculty of Engineering; and the government budget of Prince of Songkla University [grant number ENG-61-00-62-S], Thailand. The authors would like to thank Research and Development Office (RDO) and Assoc. Prof. Seppo Karrila for editing this article.

REFERENCES

1. Mwaikambo LY, Ansell MP (2002) Chemical modification of hemp, sisal, jute, and kapok fibers of alkalization. *J Appl Polym Sci* **84**, 2222–2234.
2. Asim M, Jawaid M, Abdan K, Ishak MR (2016) Effect of alkaline and silane treatments on mechanical and fibre-matrix bond strength of kenaf and pineapple leaf fibres. *J Bionic Eng* **13**, 426–435.
3. Faruk O, Bledzki AK, Fink H, Sain M (2012) Biocomposites reinforced with natural fibers: 2000–2010. *Prog Polym Sci* **37**, 1552–1596.
4. Cui Y, Lee S, Tao J (2008) Effects of alkaline and silane treatments on the water-resistance properties of wood-fiber-reinforced recycled plastic composites. *J Vinyl Add Tech* **14**, 211–220.
5. Obaid N, Kortschot MT, Sain M (2018) Predicting the stress relaxation behavior of glass-fiber reinforced polypropylene composites. *Compos Sci Technol* **161**, 85–91.
6. Younes MF, Rahman MAA (2016) Tensile relaxation behavior for multilayers fiberglass fabric/epoxy composite. *Eur J Mater* **3**, 1–13.
7. Wang Y, Cao J, Zhu L (2011) Stress relaxation of wood flour/polypropylene composites at room temperature. *Wood Fiber Sci* **43**, 262–270.
8. Bajwa DS, Bajwa SG, Holt GA (2015) Impact of biofibers and coupling agents on the weathering characteristics of composites. *Polym Degrad Stab* **120**, 212–219.
9. Mantia FPL, Morreale M (2008) Accelerated weathering of polypropylene/wood flour composites. *Polym Degrad Stab* **93**, 1252–1258.
10. Boukettay S, Almaskari F, Abdala A, Alawar A, Daly HB, Hammami A (2015) Water absorption and stress relaxation behavior of PP/date palm fiber composite materials. In: Chouchane M, Fakhfakh T, Daly HB, Aifaoui N, Chaari F (eds) *Design and Modeling of Mechanical Systems – II*, Lecture Notes in Mechanical Engineering, Springer, Cham., pp 437–445.
11. Wang Y, Cao J, Zhu L, Zhao G (2012) Interfacial compatibility of wood flour/polypropylene composites by stress relaxation method. *J Appl Polym Sci* **126**, E89–E95.
12. Siengchin S, Sinpayakun P, Suttiruengwong S, Asawapirom U (2010) Effect of nanofiller aspect ratio on the stress relaxation and creep response of toughened pom composites. *Mech Compos Mater* **46**, 341–348.
13. Phuhiangpa N, Ponloa W, Phongphanphanee S, Smitthipong W (2020) Performance of nano- and microcalcium carbonate in uncresslinked natural rubber composites: new results of structure-properties relationship. *Polymers* **12**, 2002.
14. Bhattacharyya D, Manikath J, Jayaraman K (2006) Stress relaxation of woodfiber-thermoplastic composites. *J Appl Polym Sci* **102**, 401–407.
15. Luo S, Cao J, Wang X (2013) Investigation of the interfacial compatibility of PEG and thermally modified wood flour/polypropylene composites using the stress relaxation approach. *BioResources* **8**, 2064–2073.
16. Siengchin S, Rungsardthong V (2012) HDPE reinforced with nanoparticle, natural and animal fibers: morphology, thermal, mechanical, stress relaxation, water absorption and impact properties. *J Thermoplast Compos Mater* **26**, 1025–1040.
17. Cheng L, Liu M (2017) Effect of chemical treatment on the stress relaxation of wood. *Chem Eng Trans* **62**, 139–144.
18. Pothan LA, Neelakantan NR, Rao B, Thomas S (2004) Stress relaxation behavior of banana fiber-reinforced polyester composites. *J Reinf Plast Compos* **23**, 153–165.
19. Homkhiew C, Ratanawilai T, Thongruang W (2014) Effects of natural weathering on the properties of recycled polypropylene composites reinforced with rubberwood flour. *Ind Crops Prod* **56**, 52–59.
20. Butylina S, Hyvarinen M, Karki T (2012) A study of surface changes of wood-polypropylene composites as the result of exterior weathering. *Polym Degrad Stab* **97**, 337–345.
21. Butylina S, Karki T (2014) Effect of weathering on the properties of wood-polypropylene composites containing minerals. *Polym Polym Compos* **22**, 763–769.
22. Turku I, Karki T (2016) Accelerated weathering of wood-polypropylene composite containing carbon fillers. *J Compos Mater* **50**, 1387–1393.
23. Spiridon I, Leluk K, Resmerita AM, Darie RN (2015) Evaluation of PLA-lignin bioplastics properties before and after accelerated weathering. *Composites Part B* **69**, 342–349.
24. Stark NM, Matuana LM, Clemons CM (2004) Effect of processing method on surface and weathering characteristics of wood-flour/HDPE composites. *J Appl Polym Sci* **93**, 1021–1030.
25. Farsi M (2010) Wood-plastic composites: influence of wood flour chemical modification on the mechanical performance. *J Reinf Plast Compos* **29**, 3587–3592.
26. Gwon GJ, Lee YS, Chun JS, Doh HG, Kim HJ (2010) Effects of chemical treatments of hybrid fillers on the

physical and thermal properties of wood plastic composites. *Composites Part A* **41**, 1491–1497.
27. Khamtree S, Ratanawilai T, Ratanawilai S (2020) Determining the optimum conditions for silane treated rubberwood flour-recycled polypropylene composites using response surface methodology. *Mater Today Commun* **24**, 100971.
28. Cao J, Xie M, Zhao G (2006) Tensile stress relaxation of copper-ethanolamine (Cu-EA) treated wood. *Wood Sci Technol* **40**, 417–426.
29. Geethamma VG, Pothen LA, Rhao B, Neelakantan NR, Thomas S (2004) Tensile stress relaxation of short-coir-fiber-reinforced natural rubber composites. *J Appl Polym Sci* **94**, 96–104.
30. George J, Sreekala MS, Thomas S (1998) Stress relaxation behavior of short pineapple fiber reinforced polyethylene composites. *J Reinf Plast Compos* **17**, 651–672.
31. Mirzaei B, Tajvidi M, Falk RH, Felton C (2011) Stress-relaxation behavior of lignocellulosic high-density polyethylene composites. *J Reinf Plast Compos* **30**, 875–881.
32. Badji C, Soccalingame L, Garay H, Bergeret A, Benezet JC (2017) Influence of weathering on visual and surface aspect of wood plastic composites: Correlation approach with mechanical properties and microstructure. *Polym Degrad Stab* **137**, 162–172.
33. Badji C, Beigbeder J, Garay H, Bergeret A, Benezet JC (2018) Correlation between artificial and natural weathering of hemp fibers reinforced polypropylene biocomposites. *Polym Degrad Stab* **148**, 117–131.
34. Chaochanchaikul K, Rosarpitak V, Sombatsompop N (2013) Photodegradation profiles of PVC compound and wood/PVC composites under UV weathering. *eXPRESS Polym Lett* **7**, 146–160.
35. Ratanawilai T, Taneerat K (2018) Alternative polymeric matrices for wood-plastic composites: Effects on mechanical properties and resistance to natural weathering. *Constr Build Mater* **172**, 349–357.